Attitude Determination and Control System for QSAT

Yuya Mimasu*, Kikuko Miyata, Tomohiro Narumi, Jozef C. van der Ha
Department of Aeronautics and Astronautics,
Faculty of Engineering, Kyushu University, Fukuoka, Japan
Phone: +81-92-802-3049, e-mail:number9@ aero.kyushu-u.ac.jp

Abstract

In Space Systems Dynamics Laboratory (SSDL) at Kyushu University, the small satellite QSAT is being developed. In order to achieve the mission objectives, the attitude must be determined and controlled precisely. One function of the Attitude Determination and Control Subsystem (ADCS) is to estimate the attitude of the satellite by means of a Sun sensor, magnetometer and gyro rate sensor. Another function is to control the attitude by using the three-axis magnetorquer. The attitude determination of QSAT is based on a combination of the Weighted-Least-Square and Kalman-filter estimation methods. The Weighted-Least-Square method uses the Sun sensor and magnetometer measurements and the Kalman-filter combines the resulting angular observations with the gyro rate measurements. The attitude control is performed by a magnetorquer on the basis of a B-dot control for the de-tumbling phase and a Proportional-Derivative (PD) control law for the normal-mode.

「QSAT における姿勢決定及び姿勢制御」

三桝裕也* 宮田喜久子 鳴海智博 Jozef C. van der Ha
九州大学大学院 工学府 航空宇宙工学専攻

概要

九州大学の宇宙機ダイナミクス研究室では、小型衛星 QSAT の開発が進められている。ミッション達成のために正確に姿勢決定及び姿勢制御を行うことが不可欠で、QSAT においては太陽センサ、磁気センサ、ジャイロセンサを用いた姿勢決定、及び磁気トルカを用いた姿勢制御を行う。最小二乗法と Kalman Filter を併用した姿勢決定法、B-dot 制御と PD 制御を使用した制御則の確立のために、独自で開発したシミュレータを用いて検証を行っており、今回はその進捗を報告する。

1. Background

In space Systems Dynamics Laboratory at Kyushu University, the micro-satellite QSAT[1] is being developed. This satellite aims at investigating the plasma physics in the aurora zone in order to better understand the spacecraft charging. Also it provides data for the comparison of in-orbit Field-Aligned-Currents with those of ground-based observations. The system-level characteristics of QSAT are shown in Table 1.

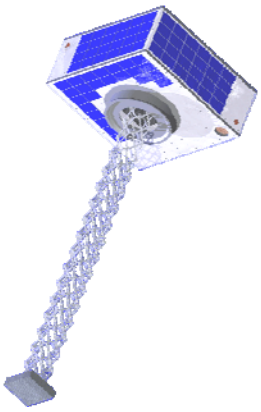

Fig. 1 QSAT Satellite

Table 1 Characteristics of QSAT

Size	480 x 480 x 300 mm
Mass	< 50 kg
Power	30 W
Attitude Control	3-axis Stabilization
Lifetime	1 year
Orbit	Sun Synchronous
Launch	H-IIA Piggy Back
Launch Date	2009 or Later

In order to achieve the mission objectives, the spacecraft attitude must be known and controlled. One function of the Attitude Determination and Control Subsystem (ADCS) is to estimate the attitude of the satellite by means of a Sun sensor, magnetometer and gyro rate sensor. Another function is to control the attitude by using the three-axis magnetorquer. Figure 2 shows the configuration of data flow within the ADCS.

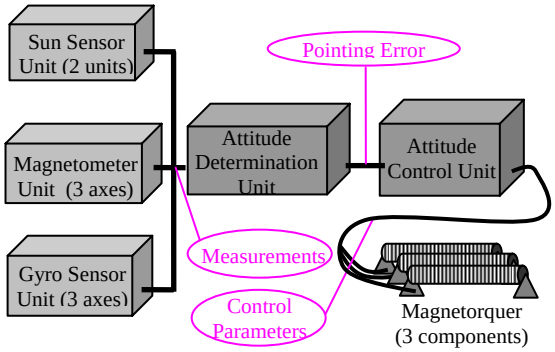

Fig. 2 Data Flow in ADCS

2. Concept of Attitude System

The ADCS must support the following operations:

① De-tumbling phase,
② Boom extension phase,
③ Normal-mode phase.

In the first phase, the ADCS controls the satellite attitude by means of the B-dot control algorithm which employs the change of the magnetic field as observed within the tumbling satellite. After the rotation rate of the satellite has been reduced, the boom is extended in the Earth direction to improve the attitude stability by means of the Earth's gravity-gradient torque.

Subsequently, the normal-mode attitude determination and control is initiated. The normal-mode attitude determination is based on a combination of the Weighted-Least-Square and Kalman-filter estimation methods. The Weighted-Least-Square method uses the Sun sensor and magnetometer measurements and the Kalman-filter combines the resulting angular observations with the gyro rate measurements. The nomal-mode attitude control is performed by the three-axis magnetorquer on the basis of a Proportional-Derivative (PD) control law.

3. Sensors

The sensor and the magnetorquer units that are part of ADCS have been completely integrated and tested at Kyushu University. The specifications of the sensors used in each unit are summarized in Table 2.

Table 2 Specifications of Sensors

Sensor	Factor	Value
Sun Sensor	Sensitivity	320~1100 (nm)
	Positioning Error	+/- 8.33 × 10^{-2} (mm)
Magnetometer	Field Range	+/- 2×10^{5} (nT)
	Resolution	40 (nT)
	Bias	2.3 %FS*
Gyro Sensor	Rate Range	+/- 100 (deg/sec)
	Resolution	0.16 (deg/sec)
	Bias	3.0 %FS*

* FS: Full-Scale

Each Sun-sensor unit (Fig.4) has three Position Sensing Devices (PSD's) on the surface plate of the satellite's body. The Sun's light can be sensed as shown in Fig. 3.

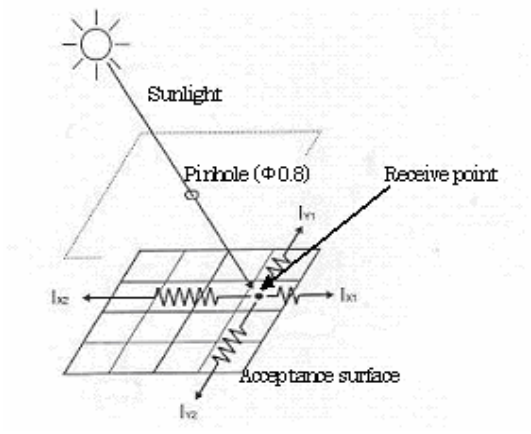

Fig. 3 Principle of Sensing the Sun's Light in PSD

The magnetometer unit (Fig.5) has the three-axis magnetic field sensor, HMC2003, produced by Honeywell Corporation. This sensor has been used by many satellites, so it has a high reliability. The sensor measures the three components of the geomagnetic field throughout the orbit. These measurements will be used by the attitude estimation process.

The gyro rate sensor unit (Fig.6) has three sensors along each axis. These sensors are produced by Silicon Sensing Device Corporation, and have mainly been used as car equipment. The sensors sense the angular rates of the satellite in inertial space. These rates will be used for the attitude propagation.

4. Actuator

The magnetorquer (Fig.7) is manufactured and tested at Kyushu University. The materials and specifications are described in Table 3.

The magnetorquer will control the satellite to the desired attitude. Although there are several disturbance torques, the satellite's residual magnetic field could be the most critical. As a measure to reduce the residual magnetic field, twisting the conductive wires will be performed. Fortunately, the on-ground tests confirm that the residual magnetism is sufficiently small.

Table 3 Specifications of Magnetorquer

Description	Value
Maximum Magnetic Moment	1 Am^2
Material of Core	PB (Ni-Fe) Permalloy
Material of Conductive Core	Cu
Number of Coils	1200

Fig. 4 Sun Sensor Unit

Fig. 5 Magnetometer Unit

Fig. 6 Gyro Rate Sensor Unit

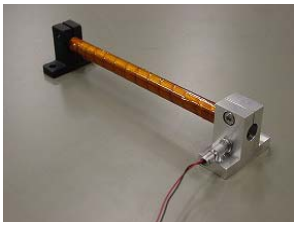

Fig. 7 Magnetorquer

5. Attitude Determination

The Weighted-Least-Square method is used to produce the best estimates of the attitude angles based on the measurements provided by the sensors at a single point of time. Subsequently, these observations are used as the inputs for the Kalman-filter as shown in Figure 8.

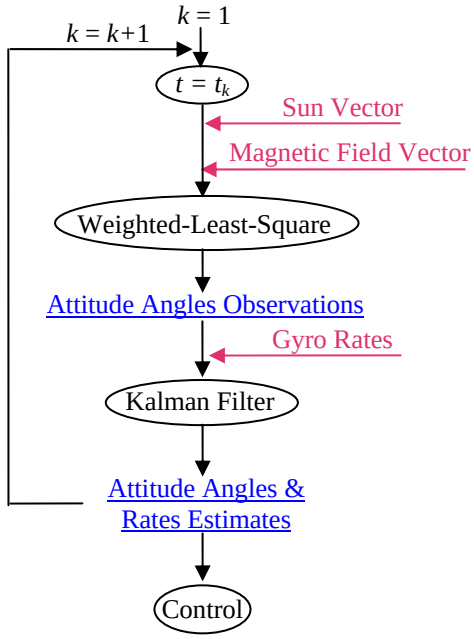

Fig. 8 Summary of Attitude Determination Logic

4.1 Weighted-Least-Square Method

In order to construct the measurement equation, the transformation between the reference frames is important. The transformation from the orbit frame to the body frame can be defined by the 3 Tait-Bryan angles, φ, θ, ψ in the 3-2-1 rotation sequence shown in Figure 9.

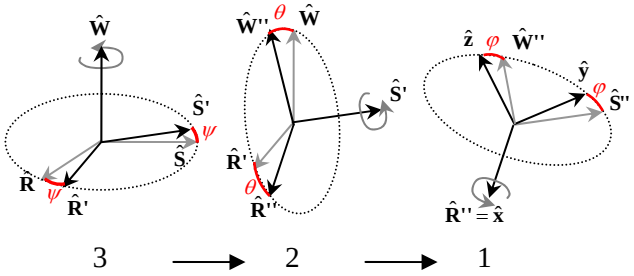

Fig. 9 Transformation from Orbit Frame to Body Frame

The measurement vector contains the Sun vector **S** and the magnetic field vector **B** and is defined as;

$$\mathbf{y} = (\mathbf{S}\,;\,\mathbf{B})^T \tag{1}$$

The transformation matrix of the measurements defined in Eq. (1) from the orbit frame to the body frame is described as:

$$\mathbf{y}^B = \begin{bmatrix} [\Psi] & 0 \\ 0 & [\Psi] \end{bmatrix} \mathbf{y}^O \tag{2}$$

where the superscripts ^{B} and ^{O} designate the measurements in the body frame and the orbit frame, respectively. The matrix $[\Psi]$ is the 3 x 3 transformation matrix in the Tait-Bryan angles φ, θ, ψ:

$$[\Psi] = \begin{bmatrix} \cos\theta\cos\psi & \cos\theta\sin\psi & -\sin\theta \\ \sin\varphi\sin\theta\cos\psi - \cos\varphi\sin\psi & \sin\varphi\sin\theta\sin\psi + \cos\varphi\cos\psi & \sin\varphi\cos\theta \\ \cos\varphi\sin\theta\cos\psi + \sin\varphi\sin\psi & \sin\varphi\sin\theta\cos\psi - \sin\varphi\cos\psi & \cos\varphi\sin\psi \end{bmatrix} \tag{3}$$

In the case when the satellite attitude is controlled, the Tait-Bryan angles (φ, θ, ψ) shown in Figure 9 can be assumed relatively small, so that Eq. (3) becomes:

$$[\Psi] = \begin{bmatrix} 1 & \psi & -\theta \\ -\psi & 1 & \varphi \\ \theta & -\varphi & 1 \end{bmatrix} \tag{4}$$

When using the transformation matrix (3), Eq. (2) becomes:

$$\mathbf{y} = \mathbf{y}^B - \mathbf{y}^O = [M]\mathbf{x} \tag{5}$$

with the state vector defined as $\mathbf{x} = (\varphi, \theta, \psi)^T$ and the measurement matrix [M] defined by:

$$[M] = \begin{bmatrix} 0 & -S_z^O & S_y^O \\ S_z^O & 0 & -S_x^O \\ -S_y^O & S_x^O & 0 \\ 0 & -B_z^O & B_y^O \\ B_z^O & 0 & -B_x^O \\ -B_y^O & B_x^O & 0 \end{bmatrix} \tag{6}$$

The measurement equation to be used in the Weighted-Least-Square model, including the measurement noise **w**, can be written as:

$$\mathbf{y}_{LS} = [M]\mathbf{x}_{LS} + \mathbf{w} \tag{7}$$

Finally, the solution of the Weighted-Least-Square, $\hat{\mathbf{x}}_{LS} = (\varphi_{LS}, \theta_{LS}, \psi_{LS})^T$ is:

$$\hat{\mathbf{x}}_{LS} = ([M]^T[R]^{-1}[M])^{-1}[M]^T[R]^{-1}\mathbf{y}_{LS} \tag{8}$$

where, $[R]$ is the covariance matrix of the measurement noise vector **w**:

$$[R] = E\{\mathbf{w} \bullet \mathbf{w}^T\} \tag{10}$$

4.2 Kalman-Filter

The Kalman-filter estimates the attitude angles and rates based on the Weighted-Least-Square observations of the angles $\hat{\mathbf{x}}_{LS}$ plus the gyro rate measurements **g**. The dynamics model is evaluated between successive measurements. The components of state and measurement vector are defined as:

$$\mathbf{y} = (\varphi_{LS}, \theta_{LS}, \psi_{LS};\ g_1, g_2, g_3)^T \tag{11}$$

Therefore, the measurement equation of the Kalman filter is:

$$\mathbf{y} = [H]\mathbf{x} + \mathbf{v} \tag{12}$$

where $[H]$ is the measurement matrix, $\mathbf{x} = (\varphi, \theta, \psi;\ \omega_x, \omega_y, \omega_z)^T$ is the state vector, g_x, g_y and g_z are the gyro rate measurements, and **v** is the process noise.

Using the kinematic equations[2] and the Euler equation, we obtain the discrete state model:

$$\mathbf{x}_{k+1} = [\Phi_k]\mathbf{x}_k + \mathbf{u}_k + \mathbf{q}_k \tag{13}$$

with the transition matrix $[\Phi_k]$ [3], the torque vector $\mathbf{u}_k$, and the integrated process noise vector $\mathbf{q}_k$ described as:

$$[\Phi_k]=\begin{bmatrix} 1 & a\Delta t_k & 0 & \Delta t_k & 0 & 0 \\ -a\Delta t_k & 1 & 0 & 0 & \Delta t_k & 0 \\ 0 & 0 & 1 & 0 & 0 & \Delta t_k \\ & & & 1 & a_x\Delta t_k & 0 \\ & \mathbf{0} & & a_y\Delta t_k & 1 & 0 \\ & & & 0 & 0 & 1 \end{bmatrix} \quad (14)$$

$$\mathbf{u}_k=\begin{bmatrix} \tau_x\Delta t_k^2/2 \\ \tau_y\Delta t_k^2/2 \\ \tau_z\Delta t_k^2/2-\Delta t_k\dot{u} \\ \tau_x\Delta t_k+a_x\tau_z\Delta t_k^2/2 \\ \tau_y\Delta t_k+a_y\tau_z\Delta t_k^2/2 \\ \tau_z\Delta t_k \end{bmatrix} \quad (15)$$

$$\mathbf{q}_k=\int_{t_{k-1}}^{t_k}[\Phi_k(\tau)]\,\mathbf{v}(\tau)\,d\tau \quad (16)$$

The a priori estimate of the system state at time t_k is denoted as $\hat{\mathbf{x}}_k^-$. The updated estimate $\hat{\mathbf{x}}_k^+$ is formed by the well known Kalman-filter formulation[4] based on the measurement, $\mathbf{y}_k$:

$$\hat{\mathbf{x}}_k^+=\hat{\mathbf{x}}_k^-+[K_k](\mathbf{y}_k-[H_k]\hat{\mathbf{x}}_k^-) \quad (17)$$

with the Kalman gain:

$$[K_k]=[P_k^-][H_k]^T\left[[H_k][P_k^-][H_k]^T+[R_k]\right]^{-1} \quad (18)$$

where $[R_k]$ is the covariance matrix of the measurement noise defined in Eq. (10). The covariance matrix $[P_k^-]$ can be expressed in the transition matrix Eq. (14):

$$[P_k^-]=[\Phi_{k-1}][P_{k-1}^+][\Phi_{k-1}]^T+[Q_{k-1}] \quad (19)$$

where, $[Q_k]$ is the covariance matrix of the system noise defined as $[Q_k]=E\{\mathbf{q}_k\bullet\mathbf{q}_k^T\}$ with the system noise defined in Eq.(16).

The update of the covariance matrix is given by:

$$[P_k^+]=([I]-[K_k][H_k])[P_{k-1}^-]([I]-[K_k][H_k])^T+[K_k][R_k][K_k^T] \quad (20)$$

The estimates of the attitude angles and rates plus their covariances are obtained by the above algorithm.

Attitude Control

In the de-tumbling mode, the satellite controls its attitude by the magnetorquers generating the magnetic moment, which reduces the time variation of the geomagnetic field vector **B**, i.e. the B-dot control low[5]. Finally, the satellite rotates only slowly about its axes. The magnetic moment generated by the magnetorquer is kept constant. Therefore the dipole magnetic moment of the magnetorquer is given by:

$$m_i=-M\,\mathrm{sgn}\left(\frac{dB_i}{dt}\right)\quad (i=x,y,z) \quad (21)$$

Before extension of the boom, the satellite must achieve a rough Earth pointing attitude which satisfies the following criteria[6], [7]:

$$\left.\begin{aligned} |\dot{\varphi}_0|&<n\frac{\sqrt{(I_y-I_z)I_x}}{I_{x0}} \\ |\dot{\theta}_0|&<2n\frac{\sqrt{(I_z-I_x)I_y}}{I_{y0}} \\ |\dot{\varphi}_0|&<\frac{\sqrt{3(I_y-I_x)I_z}}{I_{z0}} \end{aligned}\right\} \quad (22)$$

where, $\dot{\varphi}_0$, $\dot{\theta}_0$, $\dot{\psi}_0$ are the initial Tait-Bryan angular rates, I_x, I_y, I_z are the moments of inertia including the boom; I_{x0}, I_{y0}, I_{z0} are the moments of inertia without the boom, *n* is the mean orbital motion.

In the normal-mode, the satellite attitude will be controlled by employing the Proportional-Derivative (PD) control law.

Simulator

A dynamic simulator is used to produce the evolution of the attitude and the orbit under realistic torques and forces. The Two-Line-Elements (TLE), inertia moments, initial attitude angles, and the angular rates are set as inputs. After the simulation run, the sensor measurements, the attitude angles, and the angular rate follow as a function of time. In addition, the attitude control parameters produced by the controller can be input to the dynamic model in the simulator, and fed back to the process of the simulator as shown in Figure 9.

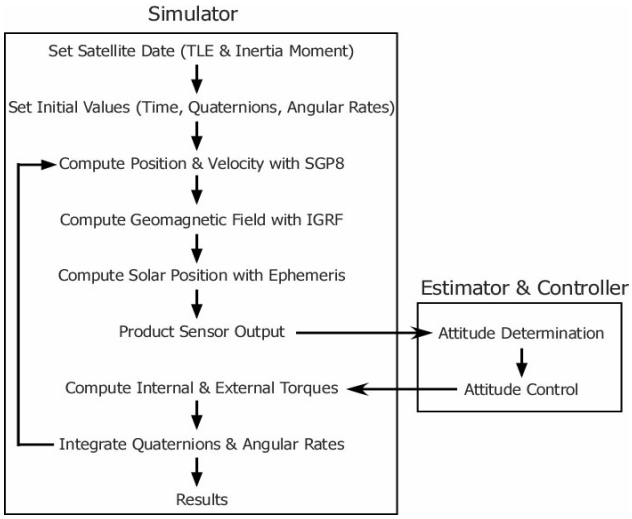

Fig. 9 Flowchart of Simulator

The attitude perturbations taken into account in the simulator are:

- Gravity Gradient[8]
- Atmospheric Drag[9]
- Solar Radiation Pressure[10]
- Residual Magnetic Moment
- Magnetic Control Torque

In addition, to model the orbit perturbations, the Simplified General Perturbation 8 (SGP8)[11] software is used. The measurements output from the simulator can be contaminated by white noise (random error) and systematic errors (biases). The white noise is produced by employing the L'Ecuyer & Box-Muller method [12].

Simulation Results

The results of the simulations of the attitude determination and control described here. At first, the difference between the estimates resulting from the estimator and the simulated attitude angles from the simulator are shown. In this simulation run, the effects of eclipse, and the attitude and the orbit perturbations are not considered. Only random noise is added to the measurements. Figures 10 and 11 show the differences of the attitude angles, and the angular rates, respectively.

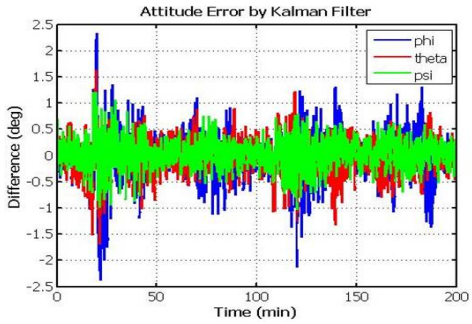

	μ (deg)	σ (deg)
Noise	0	4.03
Result	6.94×10^{-2}	0.573

Fig. 10 Difference between Estimates & Simulated Attitude Angles

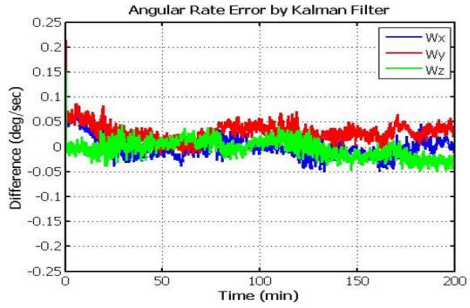

	μ (deg/sec)	σ (deg/sec)
Noise	0	2.0
Result	6.35×10^{-2}	4.17×10^{-2}

Fig. 11 Difference between Estimates & Simulated Angular Rates

.

The evolution of the angular rates in the case when the B-dot control is employed is shown in Figure 12. The perturbations and the initial conditions are described in Table 4.

Table 4 Considered perturbations & Initial Conditions

Perturbations	Gravity Gradient
	Solar Radiation
	Atmospheric Drag
	Residual Magnetic Moment (Am^2) (-0.33, -0.33, -0.33)
Control	Magnetic Moment (Am^2) (1.0, 1.0, 1.0)
	Duty Cycle: 0.5
	Initial Angular Rates (deg/sec) (30, 30, 30)

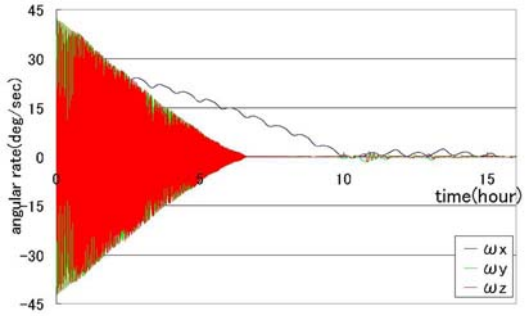

Fig. 12 Angular Rates under B-dot Control

Conclusions

In this paper, the design of the attitude determination and control system of QSAT is presented. It is shown that the Kalman filter decreases the effect of the random noise, and that the satellite rotation during the initial tumbling phase can be reduced by employing the B-dot control.

References

[1] Hanada, T., QSAT project team, "QSAT the Satellite for Polar Plasma Observation," *UN/ESA/NASA Workshop on BSS and IHY 2007*, 2007

[2] Wertz, J. R. (Editor), Spacecraft Attitude Determination and Control, Kluwer Academic Publishers, Netherland, 1978, Part III, pp.511-515.

[3] van der Ha, J., 'Initial Attitude Determination for the HIPPARCOS Satellite', Acta Astronautica, Vol.15, No.6/7, 1987, pp.421-433.

[4] Gelb, A. (Editor), Applied Optimal Estimation, The MIT Press, Massachusetts Institute of Technology, Cambridge, Massachusetts, 1974, pp.107-110.

[5] Philippe Landiech, "Extensive use of magnetometers and magnetotorquers for small satellites attitude estimation and control," 18th Annual AAS Guidance and Control Conference, Keystone, Colorado, February 1-5, 1995, AAS95-012

[6] Hosokawa, S., Hayashi, T., Takezawa, S., Haneji, K., "Effective Attitude Control System for Small Satellite" T. SICE, Vol.42, No.2, pp.123-128, February 2006 (in Japanese).

[7] Hosokawa, S., Hayashi, T., Takezawa, S., Haneji, K., "Attitude Control for the Whale Ecology Observation Satellite", IEICE Technical Report,103,SANE 2003-91, pp.37-42 (in Japanese).

[8] van der Ha, J. C., "Model of Gravity Force and Gravity Gradient Torque, FLK-SIM-TN-ZAR-004 Issue 1, April, 2006.

[9] J.M. Picone, A.E. Hedin, D.P. Drob, and A.C. Aikin, "NRL-MSISE-00 Empirical Model of the Atmosphere: Statistical Comparisons and Scientific Issues," *J Geophys. Res.*, in press 2003.

[10] Montenbruck, O., Gill, E., Satellite Orbits, Springer-Verlag, Berlin, Heidelberg, 2nd Printing, 2001, pp.77-79.

[11] Hoots, F.R. and Roerich., R.L., Spacetrack Report NO.3 – Models for Propagation of NORAD Element Sets, December 1980.

[12] Press, W. H., et al., Numerical Recepes in C++, The Art of Scientific Computing, Second Edition, Cambridge University Press, US, 2005.